

# Evaluation of Bearing Capacity of Vibro-Driven Piles from Laboratory Experiments

MICHAEL W. O'NEILL, CUMARASWAMY VIPULANANDAN, AND DANIEL O. WONG

Representative methods for predicting the bearing capacity of piles driven by vibration are described briefly, and a need to establish pile resistance prediction procedures that are based on soil properties is established. In order to investigate the influence of soil properties on piles installed by vibration, a large-scale model study was conducted in which piles were driven into a pressure chamber, to simulate in situ stress conditions, and subjected to loading tests. The soil, vibrator, and pile properties were closely controlled. Methods were developed from pile mechanics considerations and the test data (a) to predict pile capacity and (b) to select vibrator characteristics to drive piles of known target capacities. These methods are expressed in the form of simple equations that can be applied by designers having appropriate knowledge of soil, pile, and vibrator conditions. Whereas every attempt was made in the laboratory study to simulate field conditions, field verification and calibration of the capacity prediction methods are necessary before they can be applied in practice.

The driving of piles by vibration is favored by many contractors, since the installation process generally requires less time than installation by impact driving, especially in cohesionless soils. It is not uncommon for a 60- to 70-ft-long pile to be installed in less than 5 min with vibration, whereas a similar pile driven by impact may require 15 to 30 min to install.

A schematic of a typical pile-driving vibrator, or "vibro-driver," is shown in Figure 1. The vibrator employs counter-rotating masses, or an equivalent mechanism, to produce dynamic forces. In some systems, a bias mass that is isolated from the mass of the vibrator by soft springs is used to provide additional static bias load to assist in penetration. The vibro-driver forces are transmitted to the head of the pile through some type of connection, usually a chuck or hydraulic clamp, which affords an opportunity for energy loss, much as cushioning systems produce energy losses during impact driving. The pile, in turn, resists the applied forces by a combination of shaft and toe resistance that may deviate from the patterns of resistance developed during impact driving.

An impediment to the use of vibratory drivers has been the inability of designers to verify the bearing capacity of installed piles in the manner afforded by wave equation analysis of impact-driven piles. Consequently, current accepted practice consists of restriking of vibro-driven piles with an impact ham-

mer to verify static capacity calculations by means of wave equation analysis or by direct dynamic monitoring. This field procedure is counterproductive to the contractor's progress.

## PREDICTIVE FORMULAE

In the past, some notable attempts have been made to develop driving formulae to predict the capacity of vibro-driven piles without restriking the piles. Several representative examples are described briefly below.

### Snip Formula

This empirical formula is used in Soviet practice and is predicated on observed behavior of full-sized piles in the Soviet Union (1):

$$Q_t = \lambda \left( \frac{25.5 P}{A_o f} + W_t \right) \quad (1)$$

where

$Q_t$  = ultimate, static, compressional bearing capacity of pile, in kN;

$P$  = power used by vibrator to drive pile, in kilowatts;

$A_o$  = displacement amplitude of vibrator, in cm;

$f$  = frequency of vibrator, in Hz;

$W_t$  = total weight (force) of vibrator and pile, in kN; and

$\lambda$  = empirical coefficient reflecting the influence of driving on soil properties (e.g., in Soviet practice  $\lambda$  is taken to be equal to 5 in cohesionless soils).

### Davisson's Energy Balance Formula

Davisson's formula (2) is the vibratory equivalent of the modified Engineering News formula for impact-driven piles, in that it is based on an energy balance (energy supplied = energy used + losses). It was specifically developed for piles driven with resonant drivers and may be expressed in the form

$$Q_t = \frac{550 P (\text{horsepower})}{(r_p + f s_t)} \quad (2)$$

M. W. O'Neill and C. Vipulanandan, Department of Civil and Environmental Engineering, University of Houston, Houston, Tex. 77204-4791. D. O. Wong, McBride-Ratcliff and Associates, 7220 Langtry, Houston, Tex. 77040.

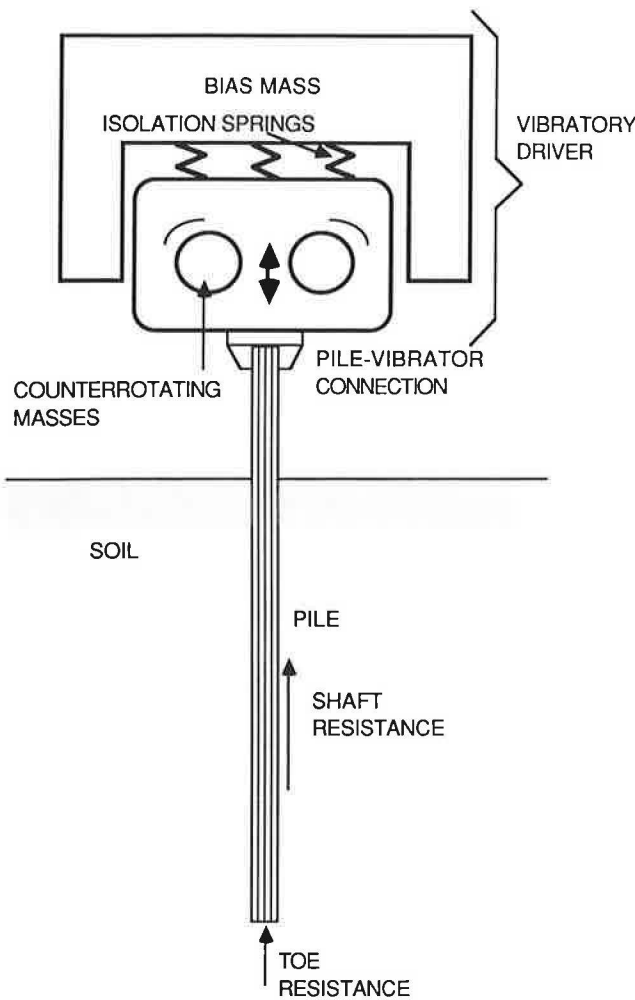


FIGURE 1 Schematic of typical vibro-driver and pile.

where

$r_p$  = rate of pile penetration, in ft/sec; and  
 $s_l$  = loss factor (equivalent set), in ft/cycle.

If the rate of penetration is high (pile capacity low), it is necessary to add another term to the numerator of Equation 2 to account for the kinetic energy of the driver. This term is evaluated as  $22,000 r_p$ . It is necessary at present to calibrate Equation 2 to specific site conditions in order to evaluate  $s_l$ . Typical values that have been used for resonant drivers (specifically, the Bodine BRD 1000) are 0.0008 to 0.008 for loose to dense cohesionless soil, respectively, with closed-ended pipe piles. Corresponding values for  $s_l$  for H piles are  $-0.0007$  to  $+0.007$ .

#### Schmid's Impulse Formula

This equation (3), appropriate in principle for low-frequency, nonresonant drivers, focuses on the impulse at the pile toe during driving. Considering the pile and vibrator as a free body, the impulse equation for one cycle of vibration, after cancellation of the impulse from the unbalanced forces from

the vibrator, becomes

$$\frac{W_b + W_v + W_p}{f} = \int_0^{T_c} Q_t dt = \alpha Q_t T_c \quad (3a)$$

where

$W_b$  = weight of bias mass (mass separated from vibrator by springs to prevent its vibrating in phase with the vibrator);  
 $W_v$  = weight of vibrator and  
 $W_p$  = weight of pile;  
 $\alpha$  = a coefficient, generally taken to be 0.67; and  
 $T_c$  = time of contact between toe and underlying soil on one cycle.

In order to evaluate  $T_c$ , one must find the minimum pile acceleration amplitude to affect penetration by means of driving tests. Acceleration amplitude in excess of this minimum acceleration (acceleration corresponding to impending refusal) is termed excess acceleration,  $a_e$ , and  $T_c$  is computed as follows:

$$T_c = \left( \frac{2 r_p}{f a_e} \right)^{0.5} \quad (3b)$$

From Equations 3a and 3b it follows that

$$Q_t = \frac{\alpha (W_b + W_v + W_p)}{f (2 r_p / f a_e)^{0.5}} \quad (3c)$$

#### Wave Equation Methods

The one-dimensional wave equation may logically be extended from impact driving to vibratory driving; however, very few published studies exist relative to this point. Chua et al. (4) describe replacing the ram, cushion, and capblock with a forcing function from a simple oscillator to model the rate of penetration of a full-scale pipe pile in a sand deposit. They indicate generally good agreement between calculated and measured penetration rates and force time histories, which suggests that, with suitable studies to calibrate the soil parameters, a wave equation approach to capacity prediction, based on vibrator properties and rate of pile penetration, may be successful in the future.

While the methods reported above and other similar methods are potentially useful, they do not explicitly incorporate fundamental soil properties, such as relative density, effective stress, and grain size. Since such properties are known to have significant effects on the capacity of impact-driven piles, it is logical that formulae that include them for the evaluation of bearing capacity of vibro-driven piles should produce more accurate predictions than formulae that do not explicitly contain their effects. The remainder of this paper describes a set of such formulae derived from large-scale laboratory tests in clean, submerged sands, in which the test piles were full-displacement, closed-ended steel pipe piles. The formula are presented in such a way as to be useful in practice, and a discussion of their applicability to field conditions follows their presentation.

## TESTING SYSTEM

Details of the laboratory testing system and observed behavior of the test piles, including their performance relative to piles driven by impact, are described elsewhere (5,6); however, a brief description of the testing system is provided here for clarity. A reusable, instrumented, closed-ended steel pipe, approximately 95 in. long and 4.00 in. in diameter, was driven with a vibrator 78 in. (or to refusal) into a pressurized sand column 30 in. in diameter, contained within a chamber. Coarse and fine uniformly graded clean sands were placed in the chamber at relative densities ranging from 65 to 90 percent. For the lower relative density, both sands were very slightly contractive and possessed angles of internal friction of 38.5 and 39.6 degrees (coarse and fine sand, respectively). For the higher relative density, both sands were dilative and possessed angles of internal friction of 42.2 and 43.6 degrees, respectively. Angles of wall friction on the steel of the test pile were 25 to 27.5 degrees for the coarse sand and 27 to 30 degrees for the fine sand, with the lower ends of the range corresponding to the lower values of relative density. Lateral effective pressures in the range of 10 to 20 psi were applied to the submerged sand column to represent mean lateral effective pressures that would be encountered in situ along the lengths of prototype piles in slightly overconsolidated, submerged sands that penetrate 50 to 100 ft. Vertical effective stresses equal to the lateral stresses and equal to twice the lateral stresses were applied to investigate the effect of  $K_0$ , the coefficient of earth pressure at rest. Drainage was provided at the lateral and upper horizontal boundaries of the sand. Controlled effective stresses were maintained at the chamber boundaries during driving and subsequent static loading tests. A schematic of the sand column is given in Figure 2.

The test pile was made of cold drawn steel tubing and had a wall thickness of 0.188 in. It was closed at the toe with a flush plate containing both a load cell and an accelerometer to measure toe performance.

The vibratory driver, which was designed and constructed specifically for this research, operated on the counterrotating mass principle. A schematic of the vibratory driver is shown in Figure 3. The rotating parts were impelled by hydraulic motors, which were in turn driven by an electrical hydraulic pump. The vibrator, which weighed 780 lb, could be configured to operate at frequencies ranging from 5 to 50 Hz (well below the resonance frequency of the test pile) with unbalanced moments of 35 to 300 in-lb and with bias mass weights ranging from 380 to 2,000 lb.

Preliminary driving tests were performed to investigate the combination of driver parameters that would produce the peak rate of penetration for the laboratory testing system. Thereafter, for all of the tests that were used in the development of the predictor equations in this paper, the vibro-driver parameters were held constant at those values:  $W_v = 780$  lb,  $W_b = 2,000$  lb,  $f = 20$  Hz (18-22), and unbalanced moment = 100 in-lb. The theoretical peak free force amplitude at the axis of the motors for these conditions was 4.1 kips.

## TEST RESULTS

The testing program was detailed. It involved investigation of power transmitted from pile head to toe, pore pressure

generation and dissipation, mode of pile penetration (e.g., rapid impulses at the toe, as suggested by Schmid), and measurement of load transfer both during driving and statically. These fundamental aspects of behavior are covered elsewhere (7,8); overall results relevant to the development of static capacity relations are given in Table 1. In that table,  $r_{pt}$  is the observed average terminal rate of penetration in the final one-pile-diameter of penetration;  $\sigma'_h$  is the horizontal effective stress maintained at the boundary of the sand column;  $d_{10}$  is the 10-percent soil particle size; and  $D_r$  is the relative density of the sand.

## BEARING CAPACITY PREDICTION AND HAMMER CHARACTERISTIC SELECTION FROM LABORATORY TESTS

The experimental data in Table 1 have been developed into analytical expressions that permit the prediction of pile capacity. These expressions are described briefly below, and procedures are described in which these expressions can be used both to predict pile capacity and to select hammer characteristics.

### Power Transfer Expressions

The bearing capacity  $Q_t$  of the vibro-driven piles correlates to several variables, including  $r_{pt}$ , absolute peak acceleration of the pile head (denoted  $a_h$ ),  $\sigma'_h$ ,  $D_r$ , and  $d_{10}$  for the driving system used in the study. Whether the pile is restruck after vibro-driving did not correlate to capacity; therefore, that effect is not included in the equation for bearing capacity. The following relationship, predicated on the power actually transferred by the vibrator to the pile head and derived from a nondimensional combination of the most significant system parameters, incorporates these variables:

$$Q_t = \frac{0.050 P_h}{r_{pt} [\beta_1(\sigma'_h) \beta_2(D_r) \beta_3(d_{10})]} \quad (4a)$$

in which  $P_h$  is the average power delivered to the pile head during the final one-diameter of penetration;  $r_{pt}$  is the average rate of penetration during the final one-diameter of penetration; and the  $\beta$  functions are empirical parameters that relate measured capacity independently to the variables indicated in the parentheses. Units for  $P_h$ ,  $r_{pt}$ , and  $Q_t$  can be any consistent set.

Equation 4a presumes rigid body behavior of the pile (i.e., zero or very small phase angle between head and toe), which is generally appropriate for prototype piles driven at low frequency (20 to 25 Hz) with lengths less than 50 ft. The dimensionless  $\beta$  factors have been determined by regression analysis of the data to be as follows:

$$\beta_1(\sigma'_h) = -0.486 + 0.0743 \sigma'_h \quad 10 \text{ psi} \leq \sigma'_h \leq 20 \text{ psi} \quad (4b)$$

$$\beta_2(D_r) = 1.96 D_r - 1.11 \quad 0.65 \leq D_r \leq 0.90 \quad (4c)$$

$$\beta_3(d_{10}) = 1.228 - 0.19 d_{10} \quad 0.2 \text{ mm} \leq d_{10} \leq 1.2 \text{ mm} \quad (4d)$$

Equation 4a, with parameters defined in Equations 4b to 4d, was found to compute the mean measured static compres-

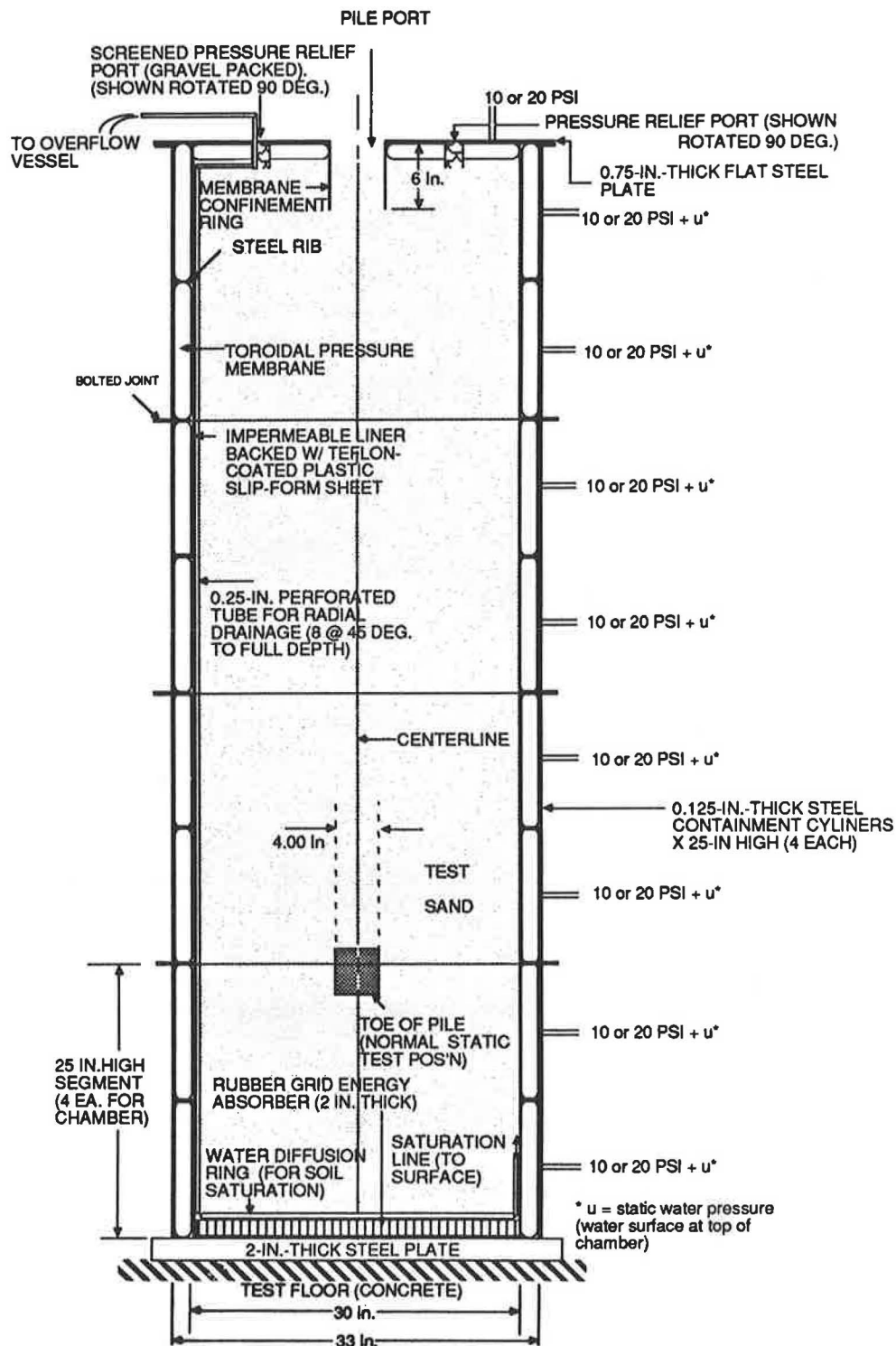


**FIGURE 2** Detailed schematic of the pressure chamber, showing lateral and vertical pressure membrane system.

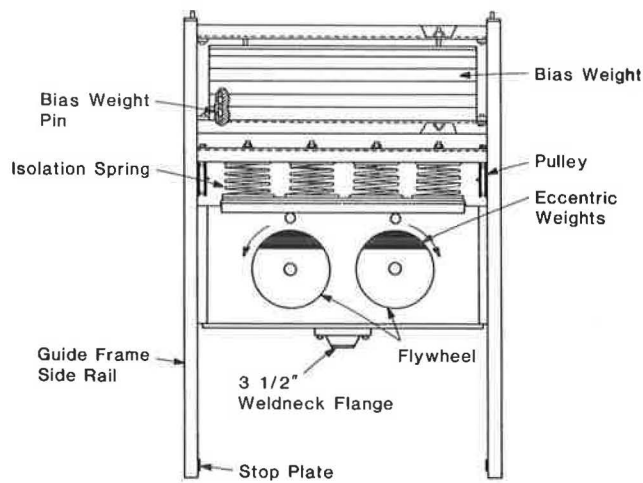


FIGURE 3 Schematic diagram of vibro-driver used in laboratory tests.

sional capacity of the vibro-driven test piles to within 1 percent, with a coefficient of variation of 12 percent.

A key parameter in Equation 4a is  $P_h$ , the power actually transmitted to the pile head during terminal penetration. The laboratory experiments revealed a strong correlation between  $P_h$ , the theoretical power of the hammer,  $P_t$ , and the absolute peak acceleration of the pile head,  $a_h$ , as follows:

$$P_h = P_t [0.25 + 0.063 a_h (g)] \quad (5)$$

It can be shown from a dynamic equilibrium analysis of the vibrator that the theoretical power  $P_t$  for a rotating-mass vibrator operating at frequency  $f$  can be obtained as

$$P_t = f \left( 4W_b + \frac{8\pi^2 f_n^2 m e}{(f_n^2 - f^2)} \right) \frac{m e f^2}{M(f_n^2 - f^2)} \quad (6)$$

where

- $m$  = combined mass of all rotating, unbalanced weights;
- $M$  = mass of the vibrator, excluding bias mass;
- $e$  = eccentricity of the rotating weights;
- $f_n$  = natural frequency of the vibrator mass-isolation spring system =  $(k/M)^{0.5}$ ; and
- $k$  = combined spring constant of the isolation springs.

Absolute peak acceleration  $a_h$  was found to correlate to soil properties and  $r_{pt}$  in the laboratory tests as indicated below:

$$a_h(g) = \alpha_1(D_r) \alpha_2(d_{10}) \left( r_{pt}^{\alpha_3(\sigma'_h)} \right), \quad (7a)$$

where  $r_{pt}$  is expressed in in./sec.

The dimensionless  $\alpha$  factors, which correlate independently the soil properties given in the parentheses to  $a_h$ , were found by regression analysis to be as follows:

$$\alpha_1(D_r) = -2.186 + 3.54 D_r, \quad 0.65 \leq D_r \leq 0.90 \quad (7b)$$

$$\alpha_2(d_{10}) = 8.99 + 2.76 d_{10}, \quad 0.2 \text{ mm} \leq d_{10} \leq 1.2 \text{ mm} \quad (7c)$$

$$\alpha_3(\sigma'_h) = 1.71 - 0.081 \sigma'_h, \quad 10 \text{ psi} \leq \sigma'_h \leq 20 \text{ psi} \quad (7d)$$

### Comparison of Capacity Prediction Methods for Chamber Tests

In order to provide some comparison of the results yielded by various predictive methods, the three methods described in this paper that employ rate of penetration as an index to capacity were used to predict the static capacity,  $Q_r$ , as a function of terminal rate of penetration,  $r_{pt}$ , in the large-scale model pile tests reported in this paper. The results are summarized in Figure 4. The intent of Figure 4 is not to suggest that the new method proposed in Equation 4a is superior to the other two methods. Equation 4a is biased to give more accurate results, since the parameters were evaluated from the reported model study. However, it is clear that the new method predicts lower rates of penetration for a given static capacity than the other two for the conditions that were studied experimentally.

### Application of Power Transfer Expressions to Bearing Capacity Prediction

Equations 4a through 7d contain implicitly the effects of the interaction of the pile, driver, and soil through the power, velocity, and acceleration terms and the soil coefficients and exponents. As with all empirical relationships, they must be considered to be valid only for the ranges of conditions modelled in the tests. The soil parameter ranges are given in Equations

TABLE 1 TEST DATA RELEVANT TO DEVELOPMENT OF STATIC CAPACITY RELATIONS

Terminal rate of penetration ( $r_{pt}$ ) (in./sec)	Horizontal effective stress ( $\sigma'_h$ ) (psi)	Ratio of horizontal to vertical effective stress ( $K_0$ )	10-percent soil particle size ( $d_{10}$ ) (mm)	Relative density of sand ( $D_r$ ) (percent)	Total penetration (diameters)	Mean static compressional capacity of pile ( $Q_r$ ) (kips)
2.1	10	1	0.2	65	19.5	13.5
3.7	10	1	1.2	65	19.5	12.0
5.5	10	1	1.2	65	19.5	12.5
0.1	20	1	0.2	90	13.8	23.5
0.1	20	1	1.2	90	18.8	38.4
0.2	10	1	0.2	90	19.5	21.0
0.4	10	1	0.2	90	19.5	25.0
0.4	10	0.5	0.2	90	19.5	17.5
0.4	10	1	1.2	90	19.5	27.0
0.7	10	1	1.2	90	19.5	24.0



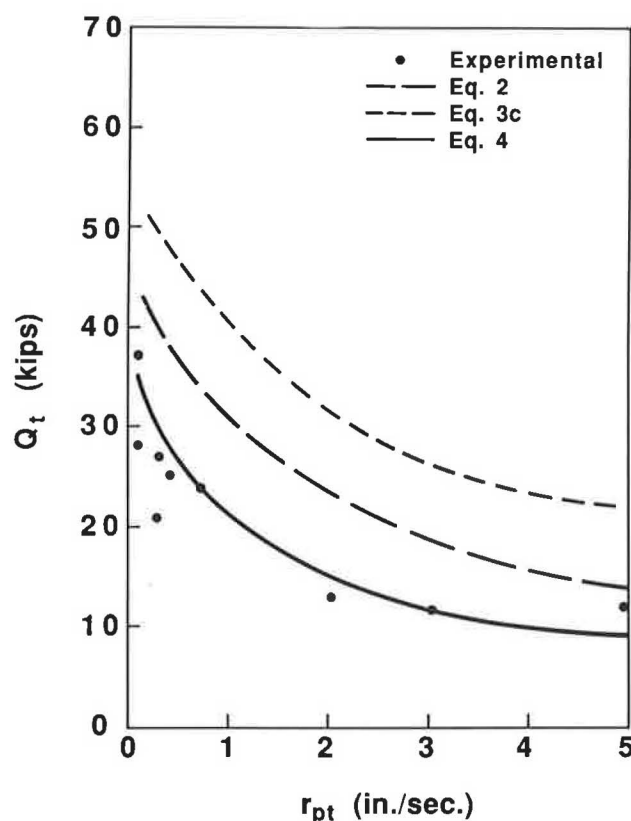


FIGURE 4 Comparison of capacity prediction methods for laboratory tests.

4a and 7a. The ranges of vibrator and pile conditions covered by the study are (1) peak single-amplitude unbalanced force developed by the vibrator was between 0.1 and 0.3  $Q_t$ ; (2) vibrator weight (excluding bias masses) was 0.15 to 0.25 times the peak single-amplitude unbalanced driver force; (3) bias weight was 0.05 to 0.10  $Q_t$ ; (4)  $f$  was the optimum frequency for driving (20 Hz in this study); and (5) the pile was closed-ended (displacement-type pile) and was driven without stopping.

It must also be considered that the power transfer equations are based on model tests in a large-sized pressure chamber and not on field tests, since field tests with appropriate measurements (acceleration time history, rate of penetration, vibrator properties, meaningful soil properties) have not heretofore been generally unavailable. The only parameter that was scaled in the pressure chamber was mean effective stress in the soil. This consideration leads to three important points:

1. Scaling of mean effective soil stress allows the relatively small model pile to represent prototypes that penetrate to depths at which the mean effective stress between the ground surface and the toe is 10 to 20 psi; that is, slightly overconsolidated, submerged sands ( $0.5 \leq K_0 \leq 1$ ) of typical unit weights to depths of 50 to 100 ft. Scaling of effective stress also reproduces the elastic and plastic properties of the soil that exist in the prototype system and that control the displacements in the pile-soil system as the pile is being driven. Vertical gradients of horizontal stress were not scaled because such scaling induces shear stresses in the soil in the chamber that do not exist in the prototype. Therefore, some judgment must be applied when selecting a single value of  $\sigma'_h$  or  $d_{10}$  in

a variable soil profile for use in Equations 4a and 7a, if these equations are to be applied to field conditions. It is tentatively suggested that, based on observations of relative resistances developed along the shaft and toe in the static loading tests in this study, single values be estimated as follows:

$$\mu = 0.67 \mu_{\text{toe}} + 0.33 \mu_{\text{middepth of pile}} \quad D_r = 65 \text{ percent} \quad (8)$$

$$\mu = 0.61 \mu_{\text{toe}} + 0.39 \mu_{\text{middepth of pile}} \quad D_r = 90 \text{ percent} \quad (9)$$

where  $\mu$  is either  $\sigma'_h$  or  $d_{10}$ . A condition not studied in the chamber tests, yet which is relatively common in the field, is that in which there is a significant change in  $D_r$  along the length of the pile, as when the pile is driven through loose soil into very dense soil. While further studies are necessary to determine the relative contributions of the toe and shaft during vibro-driving under these conditions, it is tentatively suggested that Equation 8 (in which  $\mu$  becomes relative density) be used to approximate the single value of relative density to be used in Equations 4c and 7b.

2. Since time was not scaled in the tests, the ratio of operating frequency applied to the model pile to its resonance frequency was much lower than would occur in a field prototype (approximately 0.02 in the short model and approximately 0.2 in a 75-ft-long steel pile in the field for 20 Hz excitation). This creates a model pile that behaved more rigidly than a typical prototype, although the effect is perceived to be minor, since both the model and prototype are driven at a small fraction of their resonance frequency, unless the prototype pile is either very long (>75 ft) or consists of a material that has a lower unit weight and a lower p-wave velocity than those of the steel in the model pile (e.g., timber).

3. Size also was not scaled. Thus, the laboratory test results are valid for the actual relative ratios of soil particle size to pile diameter employed in the laboratory tests, which are realistic for full-scale prototypes in medium to coarse sands. The length of the drainage path in the chamber, which scales directly to prototype drainage path length, is approximately 13 in., the distance from the pile wall to the lateral drains in the sand column. The extent to which this value is representative of field conditions and the influence of the drainage path length on prototype behavior have not been established, although the relationship of length of drainage path times soil permeability is known to affect rates of pore water pressure dissipation and, presumably, rates of penetration of piles driven by vibration.

Future field verification of the power transfer equations is therefore necessary before they can be applied to practice. Once this verification, with modification if necessary, is accomplished, it may be possible to apply the method in practice by following the step-by-step procedure outlined below:

1. Determine or estimate the relative density, average effective grain size, and mean lateral effective stress in the soil to the anticipated depth of penetration.
2. As the pile is driven, measure  $r_{pt}$ , the average velocity of penetration in the last one-diameter of penetration (or equivalent for noncircular pile).
3. Either measure  $a_h$ , the absolute peak acceleration of the pile head during the final diameter of penetration, or compute  $a_h$  from  $r_{pt}$  and the soil parameters using Equations 7a through 7d. (If power at the pile head,  $P_h$ , is actually measured during

the last one-diameter of penetration, as with a pile-driving analyzer or similar device, Steps 3 through 5 can be skipped, and the compressional capacity can be computed directly from Step 6).

4. Determine  $f$ , the frequency of operation of the hammer, and the theoretical power of the vibratory hammer at the operating frequency,  $P_t$ , either from the hammer manufacturer or from Equation 6, if the hammer is of the counterrotating mass type.

5. Determine the power actually transmitted to the pile head,  $P_h$ , either through direct measurements or by the use of Equation 5, together with the computed value of  $a_h$  (Step 3) and the relevant soil properties (Step 1).

6. Finally, compute the compressional capacity of the pile from Equations 4a through 4d.

It is presumed that any site investigation would include the recovery of samples of cohesionless soils for grain-size analysis. However, if  $\sigma'_h$  and  $D_r$  are not measured directly, appropriate correlations may be employed. For example, if the overconsolidation ratio (OCR) versus depth profile of the soil can be deduced from past geologic events,  $D_r$  can be obtained from cone tip resistances from electronic cone penetrometer soundings using correlations developed by Schmertmann (9), which can be approximated in ratio (not percentage) form, for the range of relative densities and effective stresses covered by this test program, by

$$D_r = 0.007 \frac{(q_{enc})^{0.5}}{\sigma'_v 0.33} \quad (10)$$

in which  $q_{enc}$  is the cone tip resistance in kgf/cm<sup>2</sup> for a normally consolidated sand at the depth at which the vertical effective stress is equal to  $\sigma'_v$  expressed in kgf/cm<sup>2</sup>. Thus,  $q_{enc}$  can be estimated from  $q_c$ , the measured cone tip resistance in an overconsolidated sand, from Equation 11, also proposed by Schmertmann (9).

$$q_{enc} = q_c / \{1 + 0.75 [(OCR)^{0.42} - 1]\} \quad (11)$$

In order to estimate  $\sigma'_h$  along the depth profile, one can simply compute  $\sigma'_v$  from the known position of the piezometric surface, unit weight of the soil and depth, and use a simplification of a relation proposed by Mayne and Kulhawy (10) to compute  $K_o$  as follows:

$$K_o = 0.43 (OCR)^{0.57} \quad (12)$$

Equation 12 is valid where past geologic events have not produced lower effective stresses in the ground than exist presently and for granular soils of medium to high density. Finally,  $\sigma'_h$  is computed from Equation 13 for any depth (e.g., toe or mid depth of pile).

$$\sigma'_h = K_o \sigma'_v \quad (13)$$

#### Application of Power Transfer Expressions to Selection of Hammer Characteristics

The power transfer expressions can also be used to aid in the selection of a driver. Before this can be done a target static

pile capacity must be estimated. Results of the static compressional loading tests on the piles driven by vibration in the test chamber indicated the following expression for ultimate static compressional capacity:

$$Q_t = N_o \sigma'_o A_t + \sum_{i=1}^N \beta' i \sigma'_{hi} A_{si} \quad (14)$$

where

- $\sigma'_o$  = the mean effective stress in the soil at the pile toe,
- $A_t$  = the area of the toe,
- $i$  = an index for pile segments (e.g., top half and bottom half) for shaft resistance computations,
- $A_{si}$  = the peripheral area of segment  $i$ ,
- $\sigma'_{hi}$  = the lateral effective stress in the soil in situ at the elevation of the middepth of segment  $i$  (obtained, for example, from Equation 13),
- $N_o$  = a bearing capacity parameter, and
- $\beta'$  = a shaft resistance parameter.

These latter parameters were determined from the tests in the present study to be as follows:

$$N_o = 181.1 D_r + 11.36 d_{10}(\text{mm}) - 76.1 \quad (15)$$

$$\beta' = 2.50 D_r - 0.076 d_{10}(\text{mm}) - 0.85 \quad (16)$$

Other appropriate methods for estimating static capacity can be substituted for the method described above, if such is desired.

Once the static capacity of the pile has been established, the following steps are employed:

1. A target value of terminal penetration velocity  $r_{pt}$  is selected. It is suggested that a value of 0.1 in./sec represents refusal.
2. The power required at the pile head,  $P_h$ , to produce the selected value of terminal penetration velocity is then computed from Equation 4a.
3. The peak absolute value of pile head acceleration,  $a_h$ , that would result from the above choices is estimated from Equation 7a.
4. Finally, the power required for the vibrator is computed from Equation 5.

The application of the procedure for selection of a vibrator is subject to the same constraints (ranges of variables and scaling considerations) described for estimation of static capacity. For example, once the required power is determined for a displacement-type pile, the bias weight is then set at 0.05 to 0.10  $Q_t$ , the amplitude of the unbalanced force is set at 0.1 to 0.3  $Q_t$ , and the vibrator is operated at approximately 20 Hz.

#### CONCLUSIONS

Consistent bearing capacity prediction equations were developed from a series of large-scale model tests in which displacement piles were installed in submerged sand by vibration. Constants in the model tests were vibrator and bias weight, amplitude of unbalanced force, operating frequency,

and pile characteristics (rigid, closed-ended steel pipe). Variables were focused on soil properties and included relative density, effective grain size ( $d_{10}$ ) and mean effective stress. Equations 4a through 4d were found to provide predictions of ultimate bearing capacity in varied modelled soil conditions with a coefficient of variation of 12 percent. A procedure is suggested for applying these equations to the estimation of bearing capacity of installed piles in cohesionless soils from rate-of-penetration data that involves the calculation (or direct measurement) of power transferred to the pile head. A complementary procedure is also suggested for the selection of hammer properties for piles of given design ultimate capacity. Potential users of the method are strongly cautioned that the method has not yet been verified in the field.

#### ACKNOWLEDGMENT

The study reported in this paper was supported by the National Cooperative Highway Research Program, to which the authors are indebted for permission to publish this paper.

#### REFERENCES

1. G. Steffanof and B. Boshinov. Bearing Capacity of Hollow Piles Driven by Vibration. *Proc., Ninth International Conference on Soil Mechanics and Foundation Engineering*, Vol. 2, ISSMFE, Tokyo, 1977, pp. 753–758.
2. M. T. Davisson. BRD Vibratory Driving Formula. *Foundation Facts*, Vol. 6, No. 1, 1970, pp. 9–11.
3. W. E. Schmid. *Driving Resistance and Bearing Capacity of Vibro-Driven Model Piles*. ASTM STP 444. American Society of Testing and Materials, New York, 1968, pp. 362–375.
4. K. M. Chua, S. Gardner, and L. L. Lowery, Jr. Wave-Equation Analysis of a Vibratory Hammer-Driven Pile. *Proc., Offshore Technology Conference*, Houston, Tex., Vol. 4, 1987, pp. 339–345.
5. C. Vipulanandan, D. Wong, M. Ochoa, and M. O'Neill. Modeling of Displacement Piles in Sand Using a Pressure Chamber. In *Foundation Engineering: Current Principles and Practices*, Vol. 1 (ed. F.H. Kulhawy), ASCE, New York, 1989, pp. 526–541.
6. D. O. Wong. *Driveability and Load Transfer Characteristics of Vibro-Driven Piles*. Ph.D. dissertation, Department of Civil and Environmental Engineering, University of Houston, 1988.
7. M. W. O'Neill, C. Vipulanandan, and D. Wong. Laboratory Modelling of Vibro-Driven Piles. Submitted for publication to *Journal of Geotechnical Engineering*, ASCE.
8. C. Vipulanandan, D. Wong, and M. W. O'Neill. Behavior of Vibro-Driven Piles in Sand. Submitted for publication to *Journal of Geotechnical Engineering*, ASCE.
9. J. H. Schmertmann. *Guidelines for Cone Penetration Test: Performance and Design*. Report FHWA-TS-78-209. FHWA, U.S. Department of Transportation, Washington, D.C., 1978, pp. 13–14.
10. P. W. Mayne and F. H. Kulhawy.  $K_o$ -OCR Relationships in Soil. *Journal of the Geotechnical Engineering Division*, ASCE, Vol. 108, No. GT-6, 1982, pp. 851–872.

---

*Publication of this paper sponsored by Committee on Foundations of Bridges and Other Structures.*